TECHNICAL REVIEW

No.11 / March 2019

Technical Review

MAPNA TURBINE ENGINEERING & MANUFACTURING CO. (TUGA)

TUGA

MAPNA GROUP

Willpower to Empower Generations

Cover Page:

Nowruz; Persian New Year Celebrations

Editorial

Dear Colleagues, Partners and Professionals,

A collaborative and user-centric approach has always been in place at MAPNA Turbine which put us together with our customers on the same side to bring more innovative solutions, and produce tangible bottom-line results, for the customers as well.

It is with great pleasure that a brief account of a few recent technological achievements are presented to you, our valued readers, in this edition of MAPNA Turbine Technical Review.

In the first article, the most recent MAPNA Turbine's portfolio of upgrade options available for MGT-70 heavy duty gas turbines is presented. The packages on offer, while resulting from numerous in-depth researches and technical know-how obtained over the years, are customized in close collaboration with the clients to meet their specific demands with more flexibility and higher performance.

Successful application and testing of MAPNA Group's (MECO) developed control platform 'MAPCS' through TUGA combined cycle simulator and a validated dynamic model is elaborated in the second article. As the result, the Control System has been successfully used with guaranteed functionality in PARAND combined cycle power plant.

The third article is a success story in dealing with water droplet erosion damages typically observed on the leading edges of steam turbine blades. Optimized application parameters for laser cladding of a prominent cobalt-based super-alloy are established through intensive experiments carried out on a number of specimens followed by accurate testing and lab analyses.

The fourth article introduces tailor-made, portable data acquisition system (TUGADAQ) developed by MAPNA Turbine engineers. It is an extremely effective tool for providing required operational data in our R&D initiatives, particularly experimental campaigns in the field.

Fundamental steps taken to reduce MGT-30 gas turbine environmental footprint by design and development of DLE combustor are laid out in the fifth article. Mitigation of NOx and CO emission levels was set to be the main objective of this massive R&D project, while increasing components' lifetime as the second goal. The newly developed DLE combustor has successfully undergone several tests at MAPNA Turbine Combustion Test Stand with favorable outcomes and is now set to go through final engine tests.

In the last article, meticulous steps taken to develop a comprehensive dynamic model for a common industrial gas turbine based on operational data are delineated. The developed model includes different modes of operation, having taken into account the effects of different parameters such as ambient pressure and temperature as well. Such a model is deemed essential for providing repair, maintenance and upgrading services for these engines.

Please join us in relishing the detailed account of these subjects, in this issue of the Technical Review.

Respectfully,
Mohammad Owliya, PhD
Deputy General Director

M.Owliya

MAPNA Turbine Company
(TUGA)
March 2019

Table of
Contents

Introduction

Thanks to its high availability and reliability, MGT-70 is a well-known gas turbine boasting lower maintenance costs among heavy duty gas turbines.

MAPNA Turbine has pursued a comprehensive development plan for this gas turbine platform in order to develop new products or upgrade packages with higher performance characteristics. Development features provided are based on numerous in-depth research projects and are customized in ways that meet diverse market demands raised by different customers.

As covered in previous editions of the Technical Review, MGT-70(3) is the latest commercialized version of this machine developed by MAPNA Turbine. It boasts an outstanding 185 MW of power output at 36.4% efficiency in simple cycle in standard ISO conditions. Major modifications implemented on this upgraded machine with respect to previous editions include:

- Replacement of the first 4 stages of rotary and stator compressor blades with new 3D aero
- Replacement of turbine blades and vanes at all four stages with new 3D aero, improved internal cooling paths and enhanced TBC coatings
- Replacement of compressor journal-thrust bearing with a newly designed bearing boasting higher thrust load capacity
- TBC application on some hot gas parts in combustion chamber and inner casing

1

A Portfolio of Upgrade Options on MGT-70

A schematic representation of the modifications needed on an MGT-70(3) gas turbine to have it upgraded, as well as the new Turbine Inlet Temperature (TIT) is illustrated in Fig. 1.

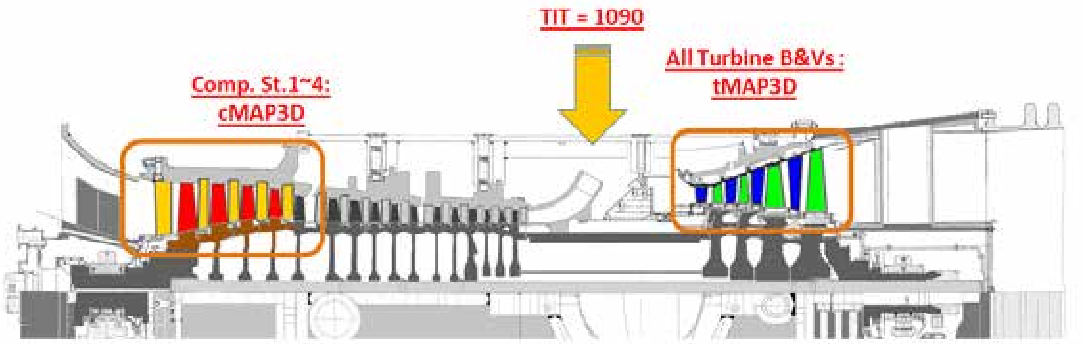

Fig. 1 – Schematic representation of major modifications to be implemented on a to be upgraded MGT-70 gas turbine

A successfully upgraded MGT-70(3) gas turbine at PARAND Combined Cycle Power Plant, south of Tehran, the capital of Iran, has accumulated over 12000 EOH so far, with acceptable performance parameters without any major operational problems.

Usually at maintenance intervals of 33000 EOH, it is necessary to replace only the first two rows of turbine blades, and blades on the third and fourth stages of the turbine are not replaced or refurbished up to 100,000 EOH. Considering this fact and to make upgrade proposals more compatible with realistic unit conditions, replacement of turbine section parts becomes limited to the blades and vanes of the first two stages. This limitation has a considerable impact on capital investments on new upgrade packages.

Taking into account the results and experiences obtained from successful MGT-70(3) upgrading projects and with the aim of decreasing capital investment, a demand-driven strategy was put in place to offer a variety of products and upgrade packages to the clients and customers to meet their specific demands while providing much more flexibility in performance characteristics.

Consequently, different proposals can be put forth based on Unique Selling Proposition (USP) approach and each individual customer's requirements.

A wide range of MGT-70(3) derivative upgrading packages, each comprising specific modifications to be implemented on the base machine to upgrade it to a more advanced version, MGT-70(3) being the latest one, is now on offer by MAPNA Turbine.

Consequently, capital investment, timeframe of the upgrading operation and subsequent performance improvements will all be contingent upon the selected upgrading packages by clients, providing a variety of upgrading options to choose from, given their specific requirements and budget.

The available upgrading options for MGT-70 gas turbine family fall into 4 major categories, listed below:

- MAP2B – T60
- MAP2B – T90
- MAP2B – CT60
- MAP2B – CT90

MAP2B is a fixed term preceding titles of all upgrading packages in the nomenclature used for this purpose. The letters "T" and "C" denote blade replacement in turbine and compressor sections, respectively. Subsequent numbers, i.e., 60 and 90 point out the maximum Turbine Inlet Temperature (TIT) in each case; 60 for 1060 °C and 90 for 1090 °C.

So, the package titled "MAP2B-CT90" incorporates modifications at both turbine and compressor sections, leading to the highest achievable TIT of 1090 °C, as is the case with MGT-70(3) gas turbine.

Performance characteristics following implementation of each upgrading package in addition to specifications of the early V94.2.3 gas turbines are listed in Table. 1.

Table 1 – Performance characteristics following the implementation of each upgrading package*

Parameter	V94.2 (Version 3)	MAP2B-T60	MAP2B-T90	MAP2B-CT60	MAP2B-CT90
Power Output (MW)	157	166	174.5	172	181
Thermal Efficiency (%)	34.4	35	35.2	35.3	35.5
Turbine Inlet Temperature (°C)	1060	1060	1090	1060	1090
Maintenance Intervals (EOH)	33000	33000	Base-mode: 33000 Life-mode: 41000	33000	Base-mode: 33000 Life-mode: 41000

* All values at ISO conditions (15 °C ambient temperature, sea level elevation, zero inlet/outlet pressure losses) with no aging effect

In the following, a more detailed description for each MGT-70(3) derivative upgrading package is provided.

MAP2B-T60

In reference to the V94.2.3 gas turbines, the early upgrading package is just limited to replacement of the first two rows of turbine blades with advanced tMAP3D blades without any subsequent rise in TIT from 1060°C. 3D airfoil design and optimized internal cooling paths in new blades result in power increase and thermal efficiency boost in turbine section.

Additionally, new blades and vanes in this package are completely retrofitted with the previous versions, so it is possible to replace these blades during Hot Gas Path Inspection (HGPI) period without removing the rotor from the casing. Also there is no need to provide hot gas path parts with Thermal Barrier Coating (TBC). Obviously, the costs associated with implementing this upgrading package with a limited scope of modification to bring about 9 MW power increase and 0.6% efficiency boost are minimal.

An illustration of the scope of modifications and TIT in the case of MAP2B-T60 upgrading package is shown in Fig. 2.

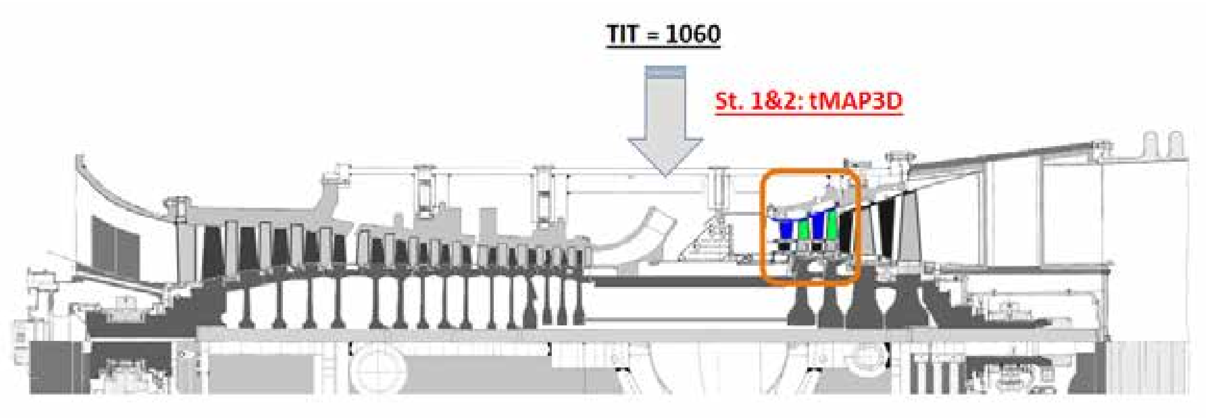

Fig. 2 – Scope of modifications in MAP2B-T60 upgrading package

MAP2B-T90

The main difference of this package from the previous one lies in implementation of TBC coating on hot gas path parts making it possible to increase the TIT up to 1090 °C, level with the MGT-70(3) gas turbine. It is necessary to apply TBC coating on the first two rows of the turbine blades, hot gas, mixing chambers and some other parts of combustion chambers to increase thermal resistance to higher TITs on these parts. So, it would be necessary to extend the scope of overhaul so as to include dis-assembly of combustion chambers and replacement of some hot section parts and components with coated ones, de-stacking the rotor to replace turbine blades with new coated tMAP3D blades as well as application of TBC coating on the hot gas inner casing or replacing it with a coated one, whichever chosen by the client.

Consequently, the power output and thermal efficiency of the upgraded machine would be increased by 17.5 MW and 0.8%, respectively, in comparison with the base V94.2.3 gas turbine.

Maintenance intervals could also be extended from 33000 to 41000 EOH as a result of using higher cooling capacity for hot section parts and components as well as application of high performance TBC coatings on these parts.

Due to significant power increase and efficiency gains resulting from implementation of this upgrading package, it might be necessary to replace generator cooler with a more efficient one to increase generator's power generation capacity. Although, this must be evaluated according to the real operating conditions of the generator.

Additionally, increase of the thrust load along the rotor resulting from power increase in gas turbine, might necessitate replacing the journal-thrust bearing of the rotor with a newly designed bearing with higher thrust load capacity developed for MGT-70(3) gas turbines.

An illustration of the scope of modifications and TIT is shown in Fig. 3 for MAP2B-T90 upgrading package.

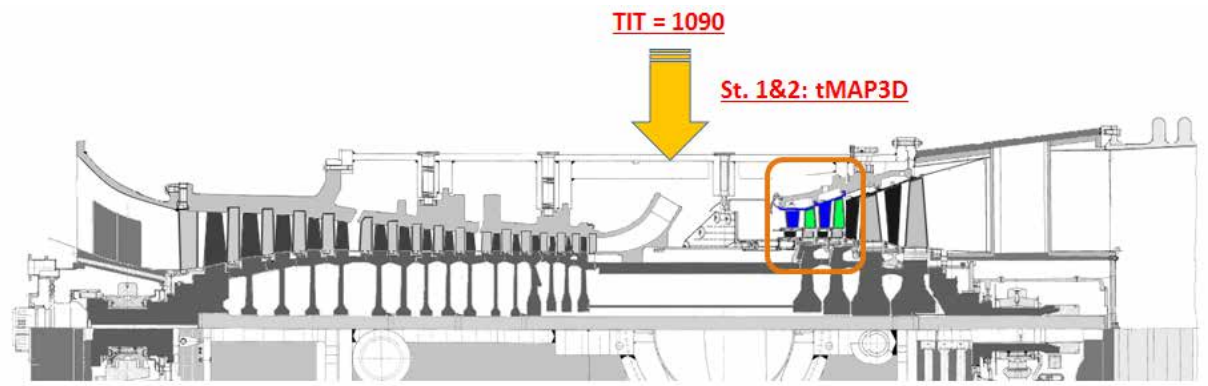

Fig. 3 – Scope of modifications in MAP2B-T90 upgrading package

[1] Diamond-Like Carbon Coating

MAP2B-CT60

As is the case with MAP2B-T60 upgrading package and notwithstanding the modifications made at the turbine section, TIT remains unchanged and equal to 1060 °C following implementation of this upgrading package. Nevertheless, the blades of the first four stages at the compressor section are replaced with newly designed cMAP3D blades as is the case with MGT-70(3) gas turbine, resulting in increased compressor mass flow rate by around 8%, with reference to V94.2.3 gas turbines. Consequently, the power output and thermal efficiency of the upgraded machine are increased by 15 MW and 0.9%, respectively, in comparison with the base V94.2.3 gas turbine.

For this upgrading package to be implemented, the structure of the air intake system and its filter configuration should be modified to meet the requirements of modified gas turbine compressor with respect to increased compressor mass flow rate.

Furthermore, the condition of the generator and its performance curve should be further investigated to make sure of its suitability for the new working conditions. For example, it might be necessary to replace or increase generator cooler capacity.

As is the case with MAP2B-T90 upgrading package and as a result of gas turbine power increase, it might be necessary to replace the journal-thrust bearing of the rotor with a newly designed bearing with higher thrust load capacity designed and developed for MGT-70(3) gas turbines.

An illustration of the scope of modifications and TIT is shown in Fig. 4 for MAP2B-CT60 upgrading package.

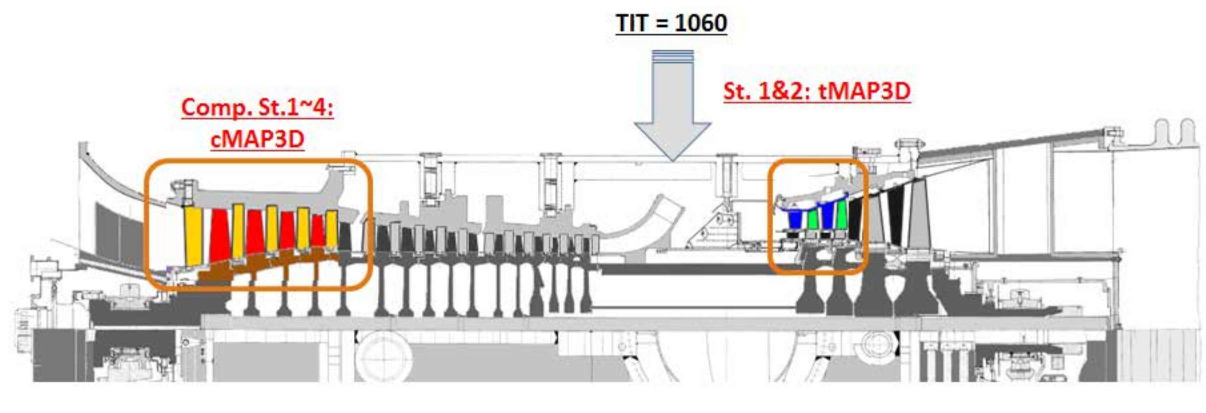

Fig. 4 – Scope of modifications in MAP2B-CT60 upgrading package

MAP2B-CT90

MAP2B-CT90 is the all-inclusive upgrading package offered by MAPNA Turbine for upgrading MGT-70 gas turbine fleet. This upgrading package comprises nearly all modifications made to develop MGT-70(3), except for the replacement of turbine blades in the third and fourth turbine stages.

So, implementation of this upgrading package would bring about almost all of the MGT-70(3) characteristics including increased mass flow rate, higher TIT, power and efficiency, as well as extended maintenance intervals.

Modifications at compressor and turbine sections as well as increase in the TIT from 1060 °C to 1090 °C, brings about increased power output of 181 MW and higher thermal efficiency of 35.5%.

All required modifications associated with MAP2B-CT90 upgrading package are listed below:

- Replacement of turbine blades at the first two stages with 3D airfoil designed tMAP3D blades boasting TBC coating and enhanced cooling schemes
- Replacement of compressor blades at the first four stages with more efficient 3D airfoil designed cMAP3D blades
- Application of TBC coating on hot parts of combustion chambers and hot gas casing
- Replacement of the rotor's journal-thrust bearing with a newly designed bearing boasting higher thrust load capacity
- Upgrading/redesigning generator cooling system and/or generator stator wiring to withstand increased power generation and hence the more demanding working conditions
- Modification of the air intake structure and its filter configuration to meet the requirements of the modified gas turbine compressor with respect to increased compressor mass flow rate

An illustration of the scope of modifications and the TIT is shown in Fig. 5 for MAP2B-CT90 upgrading package.

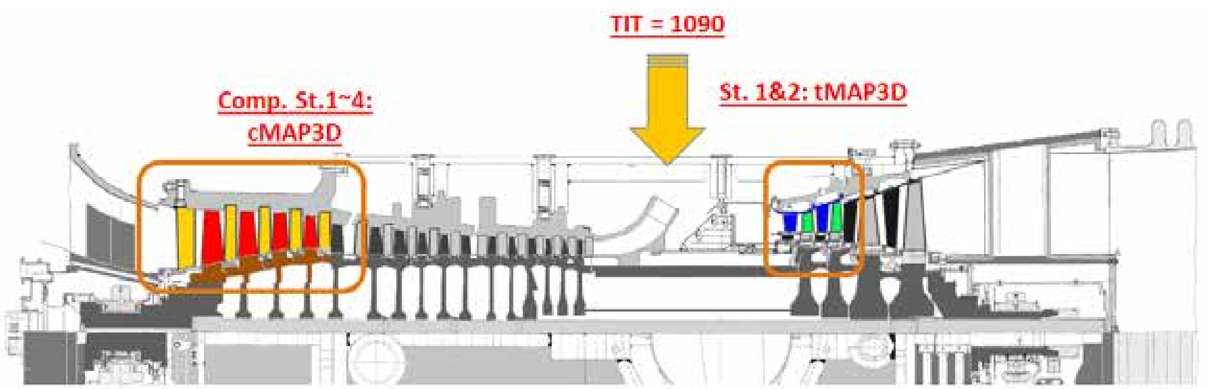

Fig. 5 – Scope of modifications in MAP2B-CT90 upgrading package

2

Successful Testing of MAPCS Control System for Combined Cycle Power Plants

Introduction

MAPNA Automation and Process Control System (MAPCS) is recognized as the state-of-the-art FCS/DCS system developed by MAPNA Electrical & Control Company (MECO). MAPCS is basically a 100% standard architecture based on FieldBus technology which is able to control all kinds of industrial processes including power plants, refineries as well as chemical, petrochemical and food industries with any degree of complexity.

The control system was used in PARAND Combined Cycle Power Plant and as is commonly practiced, it was implemented in a plant simulator to check its performance beforehand. MAPNA Turbine developed in-house simulators for gas and steam turbines with engine dynamic model as a main part.

This article presents the MAPCS structure followed by a brief description on simulator for combined cycle power plants. Then, the dynamic model extracted and verified for combined cycle simulator is presented. Last but not least, the achievements of the MAPCS project are highlighted.

MAPCS Architecture

MAPCS consists of two main parts, supervisory control platform and process control platform. supervisory control platform provides a complete set of tools for hardware connectivity, visualization, analysis and optimization of industrial data and information. process control platform which is designed and built based on the FOUNDATION Fieldbus Technology, provides required components and tools to build a powerful control system for process industries with Control-In-the-Field (CIF) capabilities, as shown Fig. 1.

FOUNDATION technology includes not only control function blocks, but also mechanisms for time management, global data access, an open and standard-based control network backbone in the form of High Speed Ethernet (HSE) and many other features that make it a reliable piece of automation infrastructure. At the same time, it is an open-source program based on international standards, allowing any automation supplier to incorporate the technology into their framework for automation while still allowing room for competitive advantages. It is essentially a standard-based template for high availability automation process that can serve as a common infrastructure for any automation process system from basic regulatory control to safety applications. MAPNA Group has exploited this new technology with the introduction of an advanced automation system released as the first generation of MAPCS.

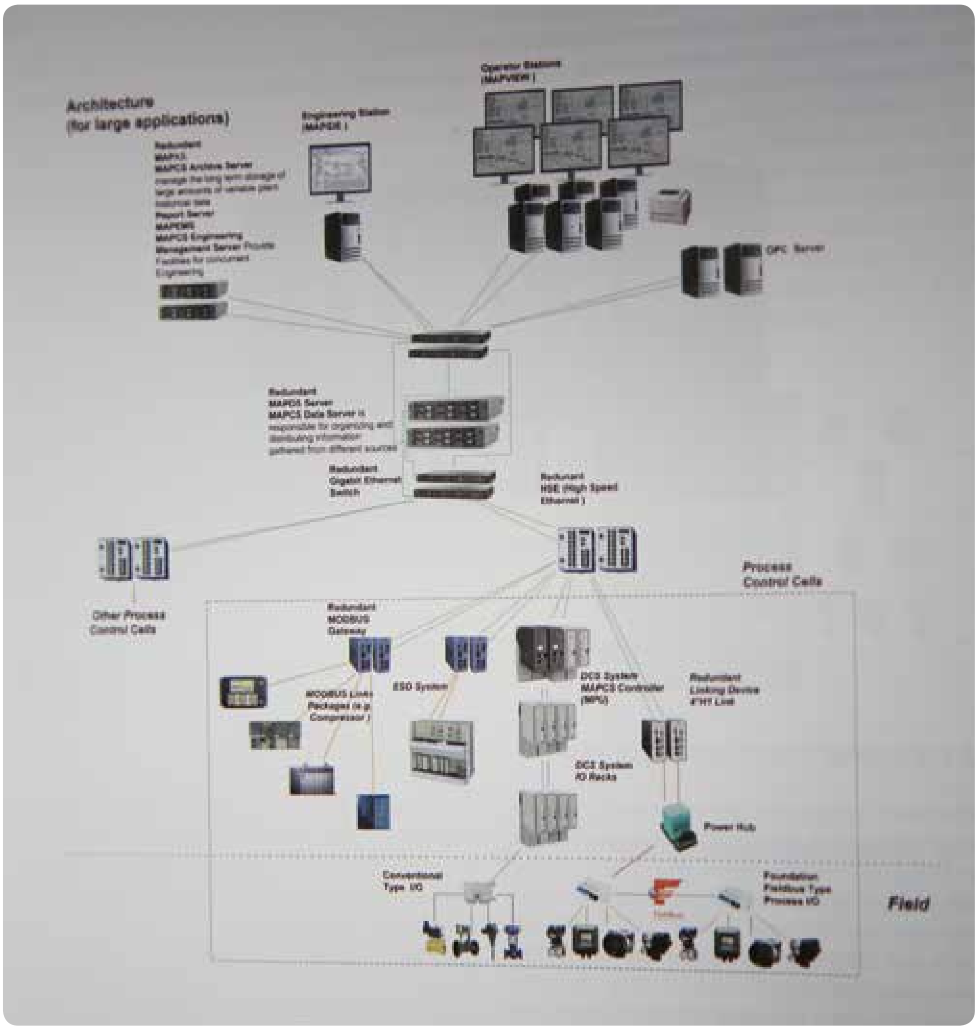

Fig. 1 – MAPCS architecture

As a scalable control system, the MAPCS uses a well-organized set of networked controllers, gateways, information servers and different types of operation and engineering clients in order to effectively control and automate a wide variety of processes with sizes varying from a few dozen to tens of thousands of control points. The rich architecture of MAPCS makes it possible for data and information to be transferred efficiently among various elements and at different layers of the system. Methods such as publisher/subscriber, synchronous and asynchronous client/server, report distribution, report by exception, etc., defined by the underlying standards such as FOUNDATION fieldbus and OPC, guarantee the optimum flow of hard and soft real-time data based on the nature of the information being transferred.

The Programmable Process Controller (PPC) shown in Fig. 2, is the main controller component of the MAPCS responsible to execute control strategies, communicate with higher layers and peer networks, e.g. HSE, Modbus/TCP as well as communicate with fieldbus devices, e.g. FF H1, and required I/O functions. The PPC supports full redundancy in processing, I/O and communications (both internal and external).

The MAPCS PPC is designed to fulfill the requirements of the most demanding process control applications. Being able to serve thousands of I/O points and the corresponding control tasks and programs, per single controller, the system can scale thousands of I/O points through a series of networked controllers using the powerful communication mechanisms built into the system's hardware and software (based on FFHSE).

Fig. 2 – MAPCS programmable process controller (PPC) unit

MAPCS Development for Combined Cycle Power Plants

The hardware, comprising 14 MAPCS panels featuring more than 4000 inputs/outputs, has been designed to provide the same functionality as that in the original system. The software has also been designed to include all functions of the control and protection systems in detail such as PIDs, drive control, set point adjuster, software switches, water and steam thermodynamic blocks, Modbus communication blocks, etc. However, this proved to be a demanding task since the function blocks of each control system is not readily available from the manufacturer. Luckily, the team managed to extract details of more than 40 function blocks by performing multiple tests on each function block.

There are over 5,000 logic pages for steam islands, including boilers, turbines and cooling as well as commands which have been implemented in the MAPCS control system. Furthermore, system parameters with an average number of 20 parameters per each function block were defined in the system.

For each function block, a series of HMI elements; known as Smart, was designed in the MAPVIEW[1] software each consisting multiple commands and feedbacks while also receiving data from the control logic system. The HMI of the control system was constructed based on connecting graphic features inside pages. In order to provide a better understanding of the complexity of the system, it should be noted that there are about 60 HMI pages for four islands, with an average of 35 Smarts per page. They all needed to be connected to the logic after being embedded in HMI pages.

Steam Plant Cycle Model

To test the MAPCS, MAPNA Turbine has developed an in-house steam plant simulator which requires dynamic model of the cycle.

Combined cycle power plant units developed by MAPNA Group typically include two Heat Recovery Steam Generators (HRSGs) downstream of a gas turbine each to recover heat energy from exhaust flow gases. The steam generated inside HRSGs is then admitted to the High Pressure (HP) and Low Pressure (LP) compartments of the steam turbine to produce power.

In order to increase the power output of the steam cycle, each boiler is also equipped with a supplementary burner providing a share of final output power of the steam cycle based on the number of burners in place as well as climatic conditions.

The rate and pressure of the steam admitted to the steam turbine is generally controlled by three hydraulic valves, i.e., governor valves. So, to provide a complete dynamic model for the steam cycle, below components are needed to be modeled:

- HRSG
- Duct Burner
- Steam Turbine
- Governor Control System

Considering the power of the gas turbine unit as an input to the model, the amount of exhaust heat energy delivered in the HRSG along with the thermal energy associated with the burner (supplementary firing) produce steam pressure. The steam pressure is then introduced to the steam turbine through the governor valves and the steam turbine power is calculated as the output of the model.

Fig. 3 shows the reference dynamic model of the steam cycle. As it is notable, this model has been split into three subsections: HRSG, steam turbine and governor.

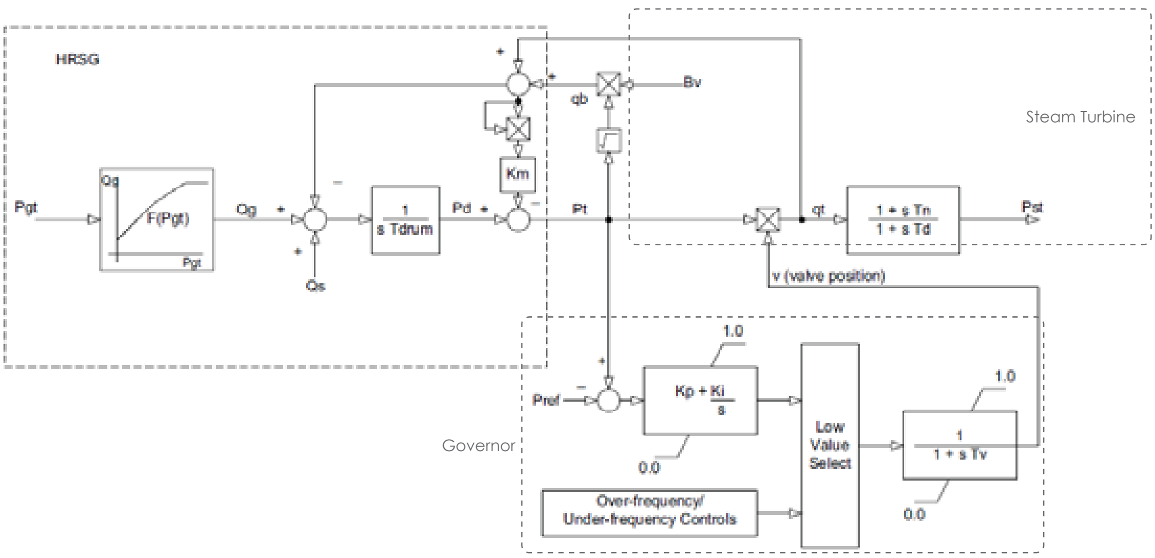

Fig. 3 – Reference dynamic model of the steam cycle

[1]An HMI software developed by MAPNA Electrical & Control company (MECO)

The HRSG model is a generic IEEE based model. In this model, a function was first used to find the equivalent thermal energy (Qg) of the gas turbine unit power (Pgt). The total heat output of this function and burner thermal energy (Qs) is given to drum dynamics which results in steam pressure (Pd). After calculation of pressure loss from the bypass flow, the final HP steam pressure (Pt) is applied to the steam turbine. Following the governor valve in the steam turbine, a transfer function is determined for LP and HP parts of turbine which together form the output power of the steam turbine (Pst).

Based on the reference model, a modified model, more similar to the process of the steam cycle, is presented in Fig. 4. In this model, two blocks of HRSG were used, with inputs from two gas turbine units. A part of this model is devoted to the governor controller for which the related parameters are implemented in accordance with the steam governor control system.

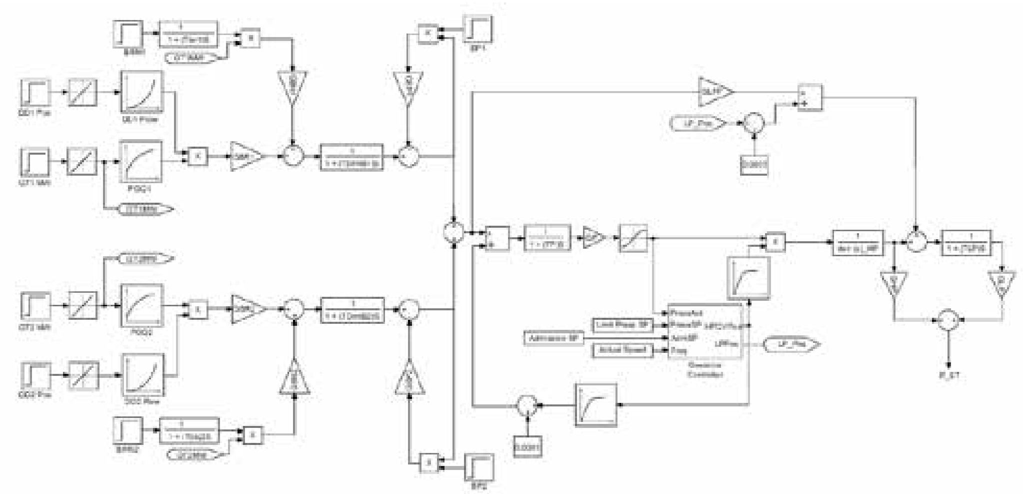

Fig. 4 – Heat cycle model developed for typical 2:2:1 configuration combined cycle power plant units

In addition to the controllers mentioned, a frequency limiting function is also considered in the governor model. Following the synchronization of the steam unit, if the network frequency goes beyond maximum and minimum thresholds, this function comes into operation for compensation of the network frequency by changing the governor valve position resulting in a change in the output power of the turbine, as shown in Fig 5.

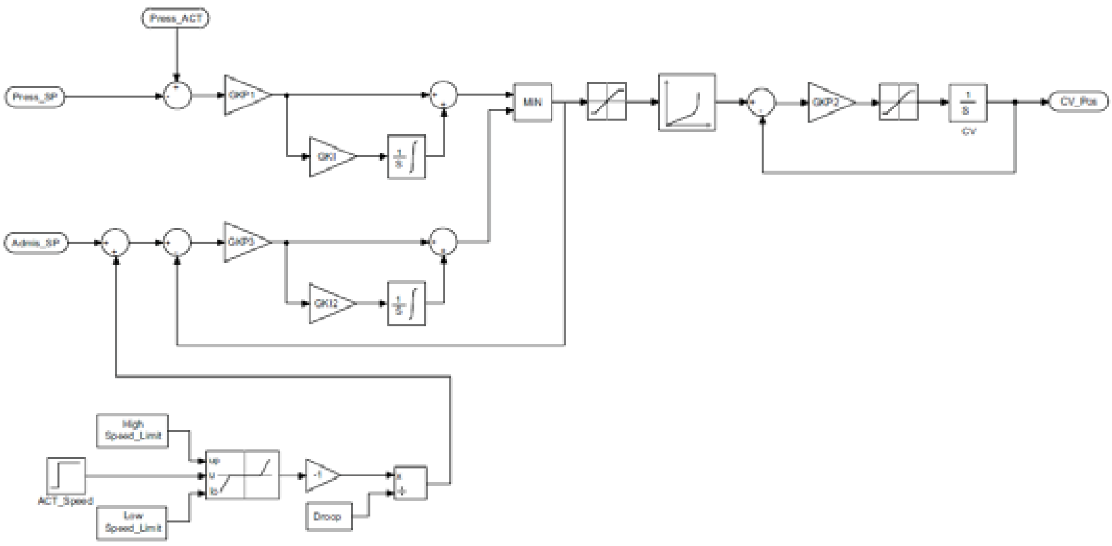

Fig. 5 – Steam turbine governor model

Model Verification

Following finalization of the steam cycle model, the outputs are validated against the actual data collected from power plants to check the accuracy of the proposed model. The maximum error encountered with the HP steam flow and pressure were 1% and 2.1%, respectively.

Moreover, the predicted power output of the model was associated with less than 2% error. It is to be noted that the outputs of the model are consistent with the actual charts and hence application of the model in a plant simulator seems extremely promising in replicating actual behavior of a power plant unit.

Combined Cycle Simulator

There are several open/close loop functions in the steam control system that should be tested in same conditions as those in the actual plant. This should be done by sending analogue and digital commands, while receiving the feedbacks in a fraction of a second to allow the control loop to be tested. For this purpose, the steam cycle simulator was developed.

The dynamic model of the steam cycle developed by MAPNA Turbine was employed in the simulator panel connected to the MAPCS boards. Some of the major tests carried out on the performance of the system include random redundancy tests of the MAPCS servers, ModBus TCP and MPUs of MAPCS cabinets. Moreover, using the simulator for the boiler and turbine island operations, below functions were evaluated successfully:

- HP drum surface control loop
- Changeover function among pumps
- Bypass pressure control loop
- Turbine over-speed test
- Random trip tests

Achievements

MAPCS steam plant project has gone through a lot of challenges in terms of engineering, construction and testing over the past three years to reach the point where it is today: Outstanding among similar projects. The system was tested on the in-house developed cycle simulator with guaranteed functionality.

This paves the way for implementation of MAPCS in steam cycle power plants in future. MAPNA Group is proud of having introduced MAPCS to the market as a domestic control platform, fully designed, manufactured and tested in PARAND combined cycle power plant.

3

Laser Cladding of Steam Turbine Blades

Introduction

One of the main damage mechanisms in steam turbine blades is Water Droplet Erosion (WDE). Investigations have shown that there is a risk of WDE occurrence in all steam paths. Studies by Byeong-eun et al. [1] indicated that the last two low pressure stages of steam turbine blades operate under wet stream conditions. In other words, the expansion of steam at these stages provides the required conditions for condensation of fine mist droplets (0.1-4 μm). Accumulation of these fine mist droplets on fixed blades results in formation of a thin layer of fluid that will move towards the leading edge of the blade by a set of mechanical factors especially inertia [2]. These droplets will gradually become larger in size (about 1 mm) and leave the surface. Subsequently, these droplets are atomized (10 - 400 μm) and collide with subsequent impinge blades by steam flow, giving rise to erosion. Hard-facing is a process in which a hard and thick layer covers the surface; this technique is one of the solutions to increase erosion resistance. Different techniques like weld overlying, plasma spray, flame spraying and laser cladding are used to deposit such a layer [3]. Laser cladding is among weld overlying methods in which a high-power laser beam is utilized as a thermal source to melt the coating materials with minimum dilution in the interface with the substrate. (Stellite™6)[1] is one of the most widely used cobalt-based superalloys showing satisfactory corrosion and erosion resistance and considerable strength properties due to the presence of Chromium and formation of various carbides. Moreover, Molybdenum and Tungsten are hardening agents that increase the strength thanks to solid solution and precipitation hardening mechanisms (carbides and intermetallic compounds) [4]. The current investigation aims at optimizing the application parameters such as laser power, feed rate, scan rate as well as percentage of transverse and vertical overlaps in fiber laser cladding of Stellite™6 coating application on leading edges of steam turbine rotary blades. It is accomplished through hardness measurement and evaluation of surface, bulk and interface properties of coating layer and substrate.

[1] Stellite™ is a registered trademark of Kennametal Inc.

Methods

Test pieces including flat plates and reduced-sized blades made of martensitic stainless steel, X20Cr13 (1.4021) were machined to have a 1.2 mm deep groove each. In fact, laser cladding of the Stellite™6 powder was accomplished when the grooves were filled. Test pieces were prepared using procedures complying with surface preparation of steam turbine rotary blades prior to laser cladding. It means that they were degreased and mechanically cleansed using emery papers (grit No. 120 to 800). Finally, all pieces were polished to Ra≈0.6 µm. The Stellite™6 with mean particle size of 50 µm was utilized as cladding material. Table 1 shows the chemical composition of this powder.

Table 1 – Chemical composition of the Stellite™ 6 powder

Elements	%Co	%Fe	%Cr	%W	%C	%Si	%Ni	%Mn
Wt.%	Balance	2.0	27.0	5.0	1.1	1.6	2.1	0.6

Cladding operations were carried out using a fiber laser as power (heat) source. A gravity-based powder feeder was used to feed the powder to the interaction zone between the laser beam and the substrate through a slide injecting nozzle. Moreover, Argon gas shielded the powder stream during the process. A four-axis Computer Numerical Control (CNC) machine was utilized to control the movement of substrate under laser beam. A schematic view of laser cladding process is shown in Fig. 1.

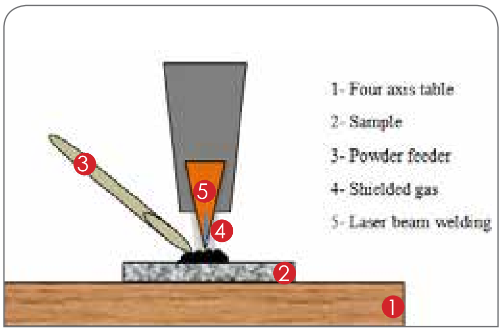

Fig. 1 – Schematic of laser cladding process

Different application parameters investigated in the present study are listed in Table 2 for all specimens.

Table 2 – Investigated laser cladding parameters for each specimen

Sample No.	Scan Rate (mm/s)	Laser Power (W)	Feed Rate (mg/s)
1	4	500	200
2	4	500	300
3	5	500	200
4	5	500	300
5	4	600	200
6	4	600	300
7	5	600	200
8	5	600	300

All cladded samples were stress relieved after two hours at 550 °C. Afterwards, only for reduced-sized blades, the laser cladded area was machined to remove all the excess coating to make it flush with the surrounding surface. To evaluate the surface and bulk condition of the cladded area, penetrant and radiographic tests were performed according to the guidelines of the ASME section V, Article No. 6. Microstructural investigations and microhardness measurements were performed using an optical microscope and Vickers microhardness tester (Micromet model, Buehler™) with a load of 300 g applied for 15 seconds according to ASTM E 384.

Results and Discussion

Laser cladding procedure was performed on prepared test pieces using parameters mentioned in Table 2. Micrographs of cladded samples' cross-sections are presented in Figs. 2 and 3.

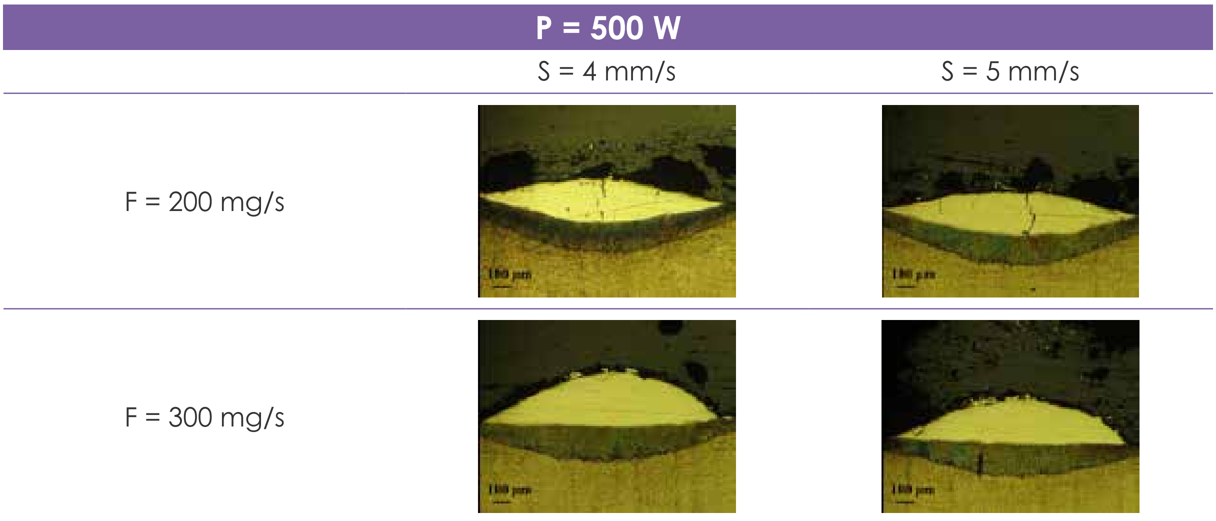

Fig. 2 – Micrographic representation of cladded samples' cross-sections for denoted parameters and laser power of 500 W

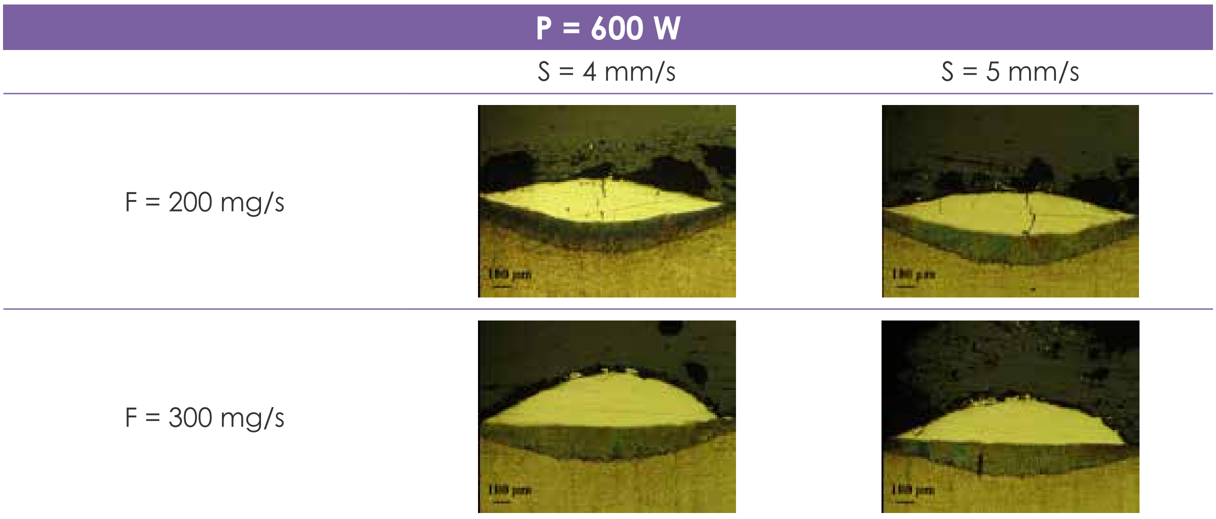

Fig. 3 – Micrographic representation of cladded samples' cross-sections for denoted parameters and laser power of 600 W

Results of single pass laser cladding of samples presented in Figs. 2 and 3 reveal that, simultaneous increase of scan rate and powder feed rate leads to geometrically abnormal coatings in case of 500 W laser power.

Moreover, higher laser power of 600 W results in extra heat input and hence excessive melting of the substrate. Although, increasing the feed rate results in improved coating geometry, chances of formation of other defects will also increases. Higher heat input in addition to low thermal conduction coefficient of the substrate leads to agitation in the interaction zone and hence formation of more and bigger porosities.

According to the results, the laser cladding parameters applied for sample No. 2, result in a coating microstructure with more appropriate dilution and free from any cracks and porosity.

In order to determine the amount of optimum transverse and vertical overlaps in multi-pass laser cladding application of the coat layer, several case scenarios were investigated on a reduced-size blade shown in Fig. 4. The application of the coating on the upper and lower parts of the blade (as shown in Fig. 4) was implemented using the parameters listed in Table 3. It is to be noted that, three passes were required to entirely fill the groove of the reduced-size blade.

Fig. 4 – Reduced-size blade used for overlap study in laser cladding application of the coating layer

Table 3 – Laser cladding parameters used for application of the coating layer on the reduced-size blade

Section	Scan Rate (mm/s)	Laser Power	Feed Rate (mg/s)	Transverse Overlap	Vertical Overlap (%)
Upper Part of the Blade	4	500	300	50	20
Lower Part of the Blade	4	500	300	60	20

Penetrant and radiographic tests demonstrate that the quality of the coating implemented is a lot more acceptable for upper half of the blade regarding the amount, type and size of the porosities.

Microstructural investigation of the cross-cut samples from both parts of the blade also suggests more satisfactory outcomes for the coating implemented on the upper half of the blade with a lot better coherence as well as fewer and smaller porosities (less than 100 µm in size), as shown in Fig. 5.

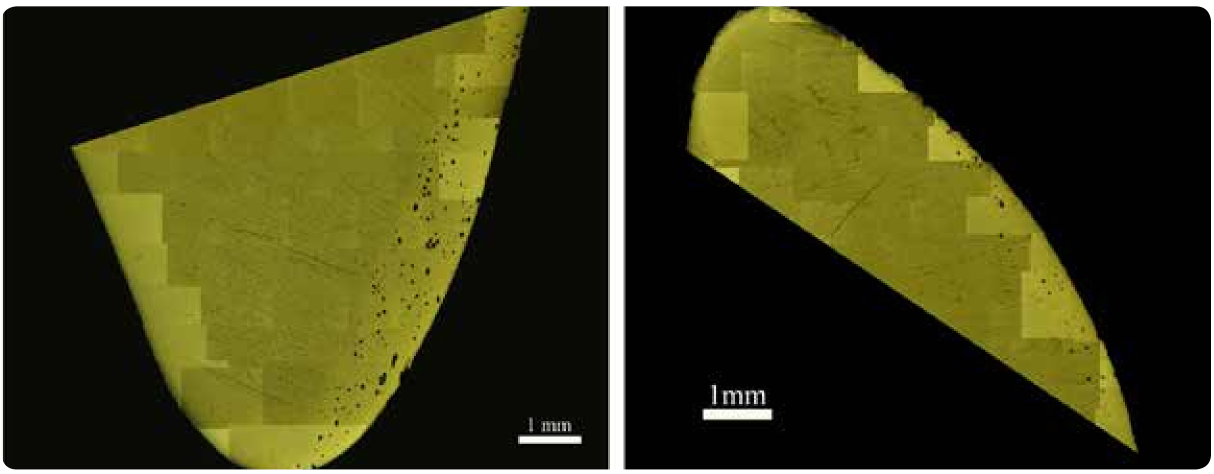

Fig. 5 – Micrographic representation at cross-sectional planes on lower (left) and upper (right) parts of the reduced-size blade

Furthermore, microhardness measurements along the coating layer points out the formation of chromium carbides ($Cr_{23}C_6$ and Cr_7C_3) in cobalt matrix with hardness values of around 700 HV0.3 compared to substrate's hardness of 450 HV0.3.

A graph of hardness values in the transverse direction along the coating layer is represented in Fig. 6.

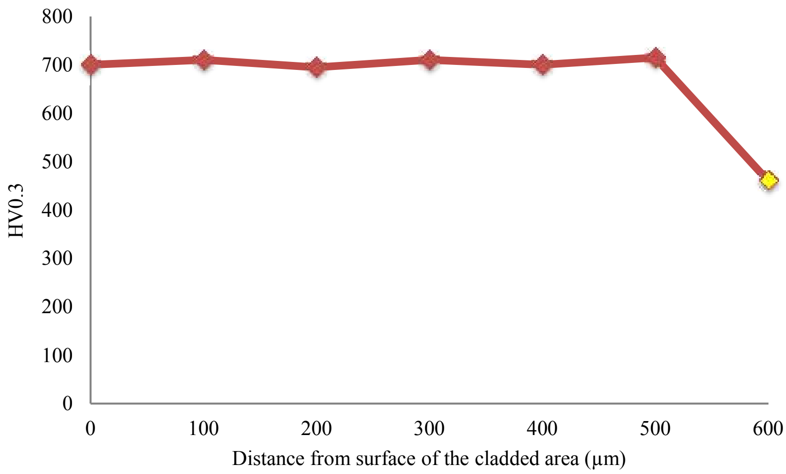

Fig. 6 – Hardness vs. distance in the transverse direction along the coating layer

Concluding Remarks

In the present study, laser cladding of Stellite™ 6 powder on X20Cr13 (1.4021) samples was investigated, and based on the results the following conclusions can be drawn:

- The optimum parameters for single pass laser cladding application of the coating layer were established as P=500 W, S=4 mm/s and F=300 mg/s
- To maintain bi-directional overlaps between passes, several different cases were studied. It was demonstrated that 50% transverse and 20% vertical overlaps yielded the most optimized results.
- Penetrant and radiographic tests in addition to microstructural evaluation and hardness measurements demonstrated that laser cladding application of the coating layer using the above-mentioned parameters leads to coatings with lower than 1% porosities that are less than 100 µm in size and hardness values of around 700 HV0.3

References

1. L. Byeong-Eun, K. J. Riu, S. H. Shin, S. B. Kwon, 'Development of a water droplet erosion model for large steam turbine blades', KSME International, Vol. (17)2003, 114-21
2. N. Yasugahira, K. Namura, R. Kaneko, T. Satoh, 'Erosion resistance of titanium alloys for steam turbine blades as measured by water droplet impingement Titanium Steam Turbine Blading', Workshop Proc. (Palo Alto, California 9–10 November 1988), 1990, 385–402
3. K. G. Budinski (1988); 'Surface engineering for wear resistance', Prentice Hall, New York, NY
4. P. A. Molian, T. S. Sudarshan (1989); 'Surface modification technologies - an engineer's guide', Marcel Dekker, New York, NY

4

MAPNA Turbine Portable Data Acquisition Modules

Introduction

Sometimes, during design or fact finding campaigns in power plants, extra process data from working plants are required. Local DCS[1] system of the plants is accessible for collecting some of the required data, but there might be some specific information which cannot be acquired through the existing data acquisition systems.

For example one may need dynamic data rather than generally static view produced by the DCS. One solution could be adding such measurements to the DCS system, but it seems not to be the proper solution, since most of these new required measurements are generally required in short term and there is no need for permanent acquisition of them in the DCS. Also, this approach needs constant re-developing, changing and upgrading of the software and hardware of the DCS system. The nature of the required signals might be so that they cannot be recorded by the DCS system which is predominantly used for recording the signals of control and protection systems of the plant rather than signal processing purposes. All these limitations make using the DCS system to serve such purposes a non-viable option. Utilizing DAQ[2] system, however, seems to be the right answer.

For large-scale typified test data acquisition projects, a stationary DAQ system is the solution. It requires stationary panels to be designed, manufactured and put in a well-suited room. The entire DAQ system will be functional and ready to operate following completion of some interconnection cabling and subsequent commissioning. This comes in handy for such projects, but what about small or medium-scale projects? What if one needs to carry out test measurements in a selection of individual plants? Although, displacing and dispatching the stationery panels and accessories from one place to another might seem a potential solution, it is surely not the first resort. To provide a better solution, MAPNA Turbine engineers and experts have designed and developed a specific DAQ system.

---

[1] Distributed Control System

[2] Common term for data acquisition systems, Data Acquisitions System is
another equivalent term

Design & Development

Main design criteria for the DAQ system were as follows:

- Multi-purpose and plant independent as much as practicable
- Easily re-configurable in the face of miscellaneous requirements
- Readily extendable according to individual project size
- Easy and fast assembly and dis-assembly to reduce required plant downtime
- Easy to transport and dispatch

Being portable, however, was not a major criterion for this project but it came about more as an inevitable outcome of the project, and an increasingly welcomed and favorable one indeed.

Two models of tailor-made DAQ systems have been developed so far. TUGADAQ-4018AS and TUGADAQ-9206IV; each with specific features and capabilities. The static DAQ system known as TUGADAQ-4018AS is capable of measuring all types of thermocouples and standard 4-20mA or ±20 mA signals. Utilizing this module, up to 64 independent channels can be sampled simultaneously.

The dynamic system known as TUGADAQ-9206IV, however, is capable of measuring up to 32 channels of voltage or current type signals with a sample rate of around 200 kHz (not simultaneous). A photograph of each model is shown in Fig. 1.

Fig. 1 – Portable DAQ Systems; TUGADAQ-9206IV (left) and TUGADAQ-4018AS (right)

The relevant software (TUGADAQ) for both modules was fully designed, programmed and tested in the R&D department of MAPNA Turbine Company. The associated software is installed on a laptop connected to the system, enabling data acquisition and processing.

A Snapshot of TUGADAQ software environment is presented in Fig. 2.

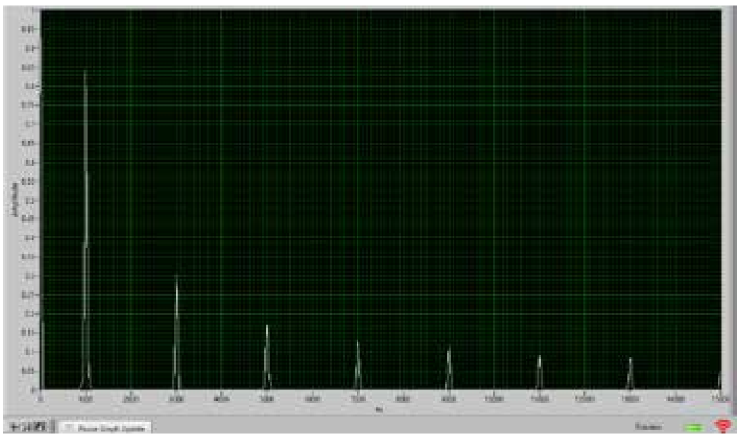

Fig. 2 – Snapshot of TUGADAQ software environment while performing online frequency domain analysis

Features

The capabilities of the specially developed DAQ systems are as follows:

- Selectable sampling rate
- Online and offline display of measurements
- Online calculation of FFT[1] in the dynamic module
- Fully time-tagged log output in the familiar MS Excel type format
- Easily re-configurable software by end users
- Easily portable package (as a luggage)
- Prefabricated, ready to use, modular interconnecting and signal conditioning parts for various types of signals. Accessories for these packages have been manufactured or chosen in a modular fashion which makes the hardware re-configuration work a lot faster and easier
- Capability of measuring loop powered or non-loop powered current type signals
- User selectable voltage input range to increase the measurement accuracy
- Embedded correction algorithms in the software for sensors calibration data
- Embedded correction algorithms in software for DAQ calibration data
- Toolkits for computing the suitable sensor calibration factors
- Easy to extend for larger-scale projects in future due to modularity in both hardware and software
- User definable online calculations on acquired signals in the software
- Configurable alarm levels for signals
- Rugged case suitable for industrial environment conditions
- Lockable case for more security as well as to protect the devices against unwanted changes and data loss

The DAQ packages are calibrated periodically using precise calibrators such as Fluke™ 753 made by Fluke Corporation).

Several data acquisition projects have been successfully accomplished using the tailor-made DAQ packages developed by MAPNA Turbine. In the future and based on likely new requirements that might arise, new features will be added to either hardware or software of these packages.

[1] Fast Fourier Transform

5

Development of DLE Combustor for MGT-30 Gas Turbine; A Fundamental Step Forward

Introduction

Gas turbine engines contribute to environmental pollution by emitting pollutants such as NOx and CO which are of special concern due to their negative impacts on human health and environment. Consequently, gas turbine manufacturers put considerable effort to reduce emission levels at the exhaust of gas turbine engines.

Generally, reduction in gas turbine pollutants emission can be achieved using different approaches including water injection, Selective Catalytic Reduction (SCR) and Dry Low Emission (DLE) combustors. However, in some plants, more water consumption is not affordable largely due to lack of water resources and hence water injection method is not feasible. Furthermore, operation of SCR systems is quite complex and expensive, requiring large amounts of ammonia.

Unlike conventional diffusion combustors, DLE systems are developed in such a way that the combustion zone temperature, as the main factor affecting emission levels, would be controlled by providing lean air/fuel mixture. In this dry emission control method, fuel and air are premixed at a specific ratio before entering the combustion zone. Obviously, development of a high-tech DLE combustor for a gas turbine requires considerable effort mainly due to design complexities and inherent operability issues of such systems.

MGT-30 gas turbine is primarily designed based on diffusion type can-annular combustor with NOx emission level of around 200 ppm at the base load. This high level of emission is not accepted according to the environmental standards and regulations in Iran and other countries where MGT-30 gas turbines are in operation. Thus, considering the target NOx emission level of 25 ppm, substitution of original combustor making use of the DLE technology was foreseen in the upgrading roadmap of this product and the process of design, prototype construction and testing of the new developed combustor is also accomplished in MAPNA Turbine.

DLE Combustor Design

From technical point of view, the main objective defined for this development project was to reduce MGT-30 gas turbine NOx emission. Increasing combustion chamber components lifetime was also considered as onother target along with the relief in thermal loading of turbine blades via combustor exit pattern factor reduction. The concept of new combustion system design is established based on the following data and constraints:

- The new combustor shall be retrofittable on operating MGT-30 gas turbine units, i.e., no change in mating geometry and position of burner flange and transition piece (TP) ending is allowed relative to the combustor casing and the first stage nozzle vane, respectively.
- Cycle parameters as design inputs are approximately the same as primary combustor. Although, a minor drop in cycle efficiency is expected due to a little increase in combustor pressure drop.

Given the fact that the design of a gas turbine combustor from scratch is a very expensive process requiring a great deal of development time, effort and investment, benchmarking from a close premixed operating combustor, helps substantially in reducing costs and risks of project and accelerates design progress, as well. Therefore, the DLE technology for MGT-30 gas turbine engines is achieved on the basis of a baseline combustor in such a way that the burner general configuration is remained unchanged and the liner is designed so as to meet the target parameters and constraints.

According to the literature, NOx production proceeds to a significant rate at primary zone temperatures of above 1850 K, while the low amount of NOx and CO formation would be achieved simultaneously at temperature range of 1700-1900 K. consequently and with regard to the target NOx & CO level of 25 ppm and 15 ppm, respectively, maximum primary zone temperature of 1850 K is selected for design process of the new DLE combustor. It is noteworthy that, in conventional diffusion combustors like those of MGT-30 gas turbine, the flame temperature reaches 2300 K which is associated with high levels of NOx emission.

To estimate the required air entering the primary zone from burner, average equivalence ratio, corresponding to the target flame temperature is calculated at design point conditions. As shown in Fig. 1, the average equivalence ratio of around 0.5 results in primary zone temperature of 1850 K.

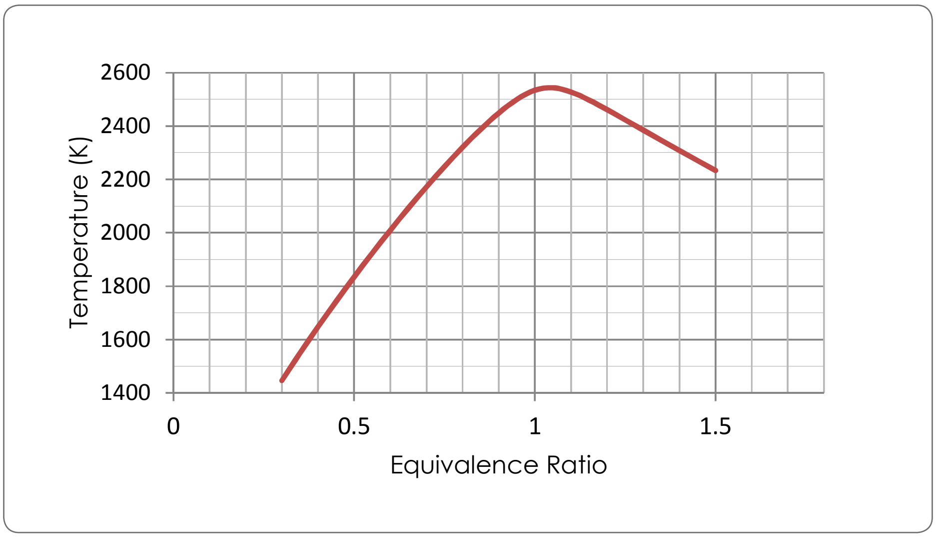

Fig. 1 – Adiabatic flame temperature vs. equivalence ratio calculated at design conditions

According to the obtained equivalence ratio and considering the combustor air and fuel boundary conditions dictated by engine cycle parameters, the new combustor's initial zonal gas temperature as well as air partitioning and liner material temperature are calculated and tuned using an in-house preliminary-phase combustor design code. Although, the required major combustor's geometrical parameters are given to the design code to setup calculations. In this phase, the main liner characteristics including cooling strategy, dilution holes and transition piece configuration are determined and required modifications are applied to the baseline combustor liner configuration to meet the design targets. The baseline burner is well-adapted to the design constraints with minor changes in its geometrical aspects.

In DLE double-channel premixed burners, the fuel is supplied via two channels of pilot and main burners and injected into the combustion chamber from distributed holes on each burner's swirler blades and hence mixed properly with combustion air. Regarding the injection location and burner channels' geometry, reactants have a good opportunity to prepare homogeneous mixture until it reaches the reaction zone. From the main burner, reactants enter the flame zone with equivalence ratio of around 0.5, while the pilot burner provides a partially premixed mixture with near stoichiometric equivalence ratio to help maintaining stability in a wide range of operating conditions.

After finalizing general combustor configuration, CAD and CAE analysis of combustor is performed using commercial software to assess designed combustor performance more precisely and optimize the geometrical aspects with the aim of bringing the results closer to design targets. In this phase, numerical simulation was performed for modeling of reactive flow field and conjugate heat transfer (CHT) calculations. The optimization process was performed using alternative geometries and pilot fuel ratios, based on variation of target parameters such as maximum flame zone temperature, pressure drop and combustor exit temperature pattern factor.

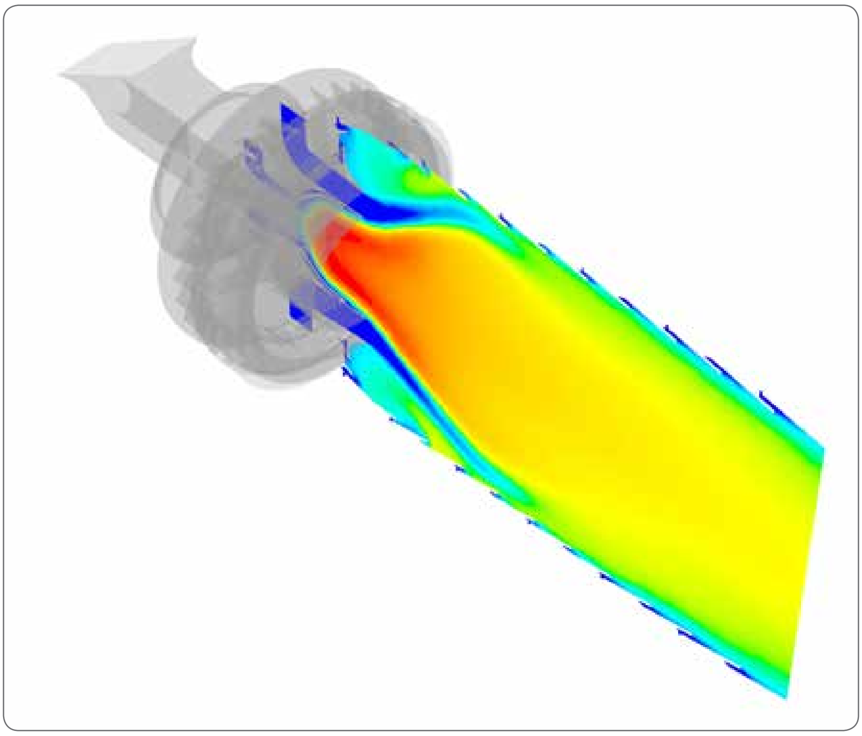

Fig. 2 –Temperature contours on the mid-plane of the developed DLE combustor

Prior to the combustor's CHT analysis, material selection process for combustor components was carried out based on expected thermomechanical conditions and supply-related issues. The selected material for most burner parts is Hastelloy, while Haynes group super alloys are selected for liner and TP parts. Also, to extend liner assembly lifetime to around 30000 EOH, thermal barrier coating is considered to be applied on inner surfaces of the liner and its thickness is determined based on TBC application approach and its requirements. According to the calculation results, the average liner material temperature reduction via TBC application is about 50 °C.

Finally, at the end of detailed design phase, 3D models and related drawings of the DLE combustor are prepared for first article construction and implementation of relevant tests.

Prototyping

In order to evaluate the new DLE combustor performance, a single burner and liner are manufactured utilizing rapid prototyping schemes to setup single burner atmospheric tests.

The parts of the DLE burner were primarily manufactured by machining of the raw materials. Due to geometrical complexity and presence of very small and precise fuel injection holes, high technology techniques such as electrical discharge drilling and laser beam welding were employed in the manufacturing process of the newly developed DLE burner.

The combustor liner also consists of various parts in cylindrical and transition piece segments that were manufactured using different technologies including sheet metal forming, machining and investment casting for geometrically complicated parts.

In order to further accelerate the project progress, time consuming investment casting procedure was replaced by additive manufacturing technology for first article testing of certain properties before serial production could begin. Additionally, utilizing this novel technology in manufacturing of the combustor liner is a remarkable step in paving the way for greater agility in design, maintenance and manufacturing of gas turbine components. Identifying requirements, pivotal challenges and knowledge acquisition of additive parts quality control make it much easier to acquire more knowledge in this innovative technology.

Fig. 3 – AM parts made for MGT-30 gas turbine DLE combustor liner

As mentioned earlier, ceramic type coating was considered for inner surfaces of the combustion liner to extend its lifetime. Although, geometrical complexity, exclusively sharp edges in the transition piece and narrow space for movement of coating devices makes it highly challenging to apply coating layer on inner surfaces of the MGT-30 gas turbine DLE combustor liner, according to the developed specification.

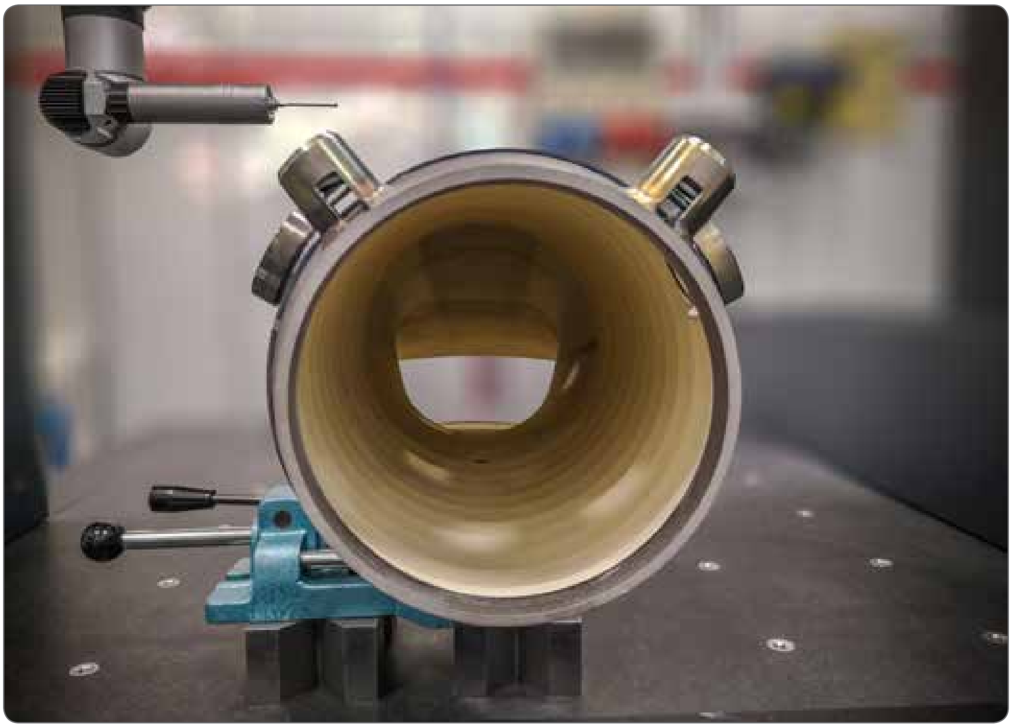

Fig. 4 – MGT-30 gas turbine coated DLE combustor liner

Single Combustor Test

Pretesting and validation of the new DLE combustor is one of the main phases during product development process that would be accomplished by performing relevant tests before finalizing the combustion system configuration. Generally, a new combustor's tests may include atmospheric, high pressure and engine tests depending on the scope of project, cost & risk assessments as well as availability of test facilities.

In the present project, the prototype tests were planned to be carried out firstly under atmospheric conditions. Regarding the possibility of engine test, those design parameters that may not be evaluated satisfactorily under atmospheric conditions such as exact emission level, dynamic instability and additive parts lifetime estimation would be assessed during field testing.

As presented previously in the Technical Review No. 6, MAPNA Turbine Combustion Test Stand has been developed to operate at low absolute pressures up to 2.5 bar and test rig air inlet temperature of up to 500 °C. The test rig module has been designed and constructed based on 1/16th of the MGT-30 gas turbine combustor to provide the possibility of the DLE combustor testing.

Fig. 5 – MAPNA Turbine atmospheric combustion test stand

The main parameters evaluated via single burner tests are ignitability, combustion chamber pressure drop, combustor exhaust gas temperature profile, NOx and other pollutants emission, as well as flame stability.

Obviously, some measured parameters with high pressure dependency, need to be corrected to stand for engine operating conditions using available experimental correlations and accuracy of these correlations for the present combustor test will be verified following implementation of engine tests.

One of the most important tests for a new combustor is related to its ignition characteristics. The combustion chamber pressure at turbine startup is close to the atmospheric pressure, which allows providing testing conditions approximately the same as the actual engine performance engine conditions in the laboratory. Having known the GT startup fuel flow rate and other cycle parameters, the DLE combustor ignition test performed using MGT-30 ignition system mounted on the test rig. As explained before, in GT startup the fuel gas would be supplied into the pilot channel of DLE burner and this concept is followed in these tests.

The DLE combustor ignition performance was characterized, having high reliability around engine ignition point and as expected, successful ignition is much sensitive to the amount of combustor inlet air and corresponding flow velocity rather than fuel flow rate. As a result, the engine ignition performance may be improved by changing the start position toward lower rotor speeds, if needed.

During the tests, the optimal value of pilot to main fuel ratio (PFR) achieved by running various tests at the DLE combustor base-load conditions with different PFR values. Accordingly and by comparing the results of emissions, temperature pattern factor and flame stability, limited acceptable range of PFR determined with maximum NOx emission of 25 ppm calculated for engine pressure condition. The optimum value of PFR will be selected to be applied on GT control system based on the new combustor's engine test results. The representative combustor exit temperature distribution at PFR value of 20% is depicted in Fig. 6.

During DLE combustion system design procedure, two alternative designs regarding liner dilution holes determined to be finalized according to the test results. The first alternative was a liner without any dilution holes and the second was a liner with two opposite dilution holes with the same diameter calculated during the design phase.

Accordingly, the first article liner constructed without dilution holes and the required tests at design point conditions accomplished using this liner as the first alternative. Afterward, two dilution holes with specified diameter were drilled in predetermined positions on the liner and similar tests were performed.

Based on tests data analyses, the overall combustor performance with both alternatives is satisfactory and the only observed differences are related to minor changes in combustor exit temperature pattern factor and NOx emission levels. By comparing the test results and considering the influence of each alternative on GT performance, the second alternative is selected to be applied on the first DLE combustor set for going through the engine test.

The final phase of this project is manufacturing one set of the developed combustor and evaluating its performance in real GT conditions. The required modifications in the GT control system, fuel skid and P&ID will be performed and finalized during the DLE combustor engine tests. Besides MGT-30 gas turbine performance parameters, a series of assessments and final evaluations will be carried out regarding the lifetime (especially additively manufactured parts), DLE combustor emission levels and combustor operability issues on the engine at different operating conditions.

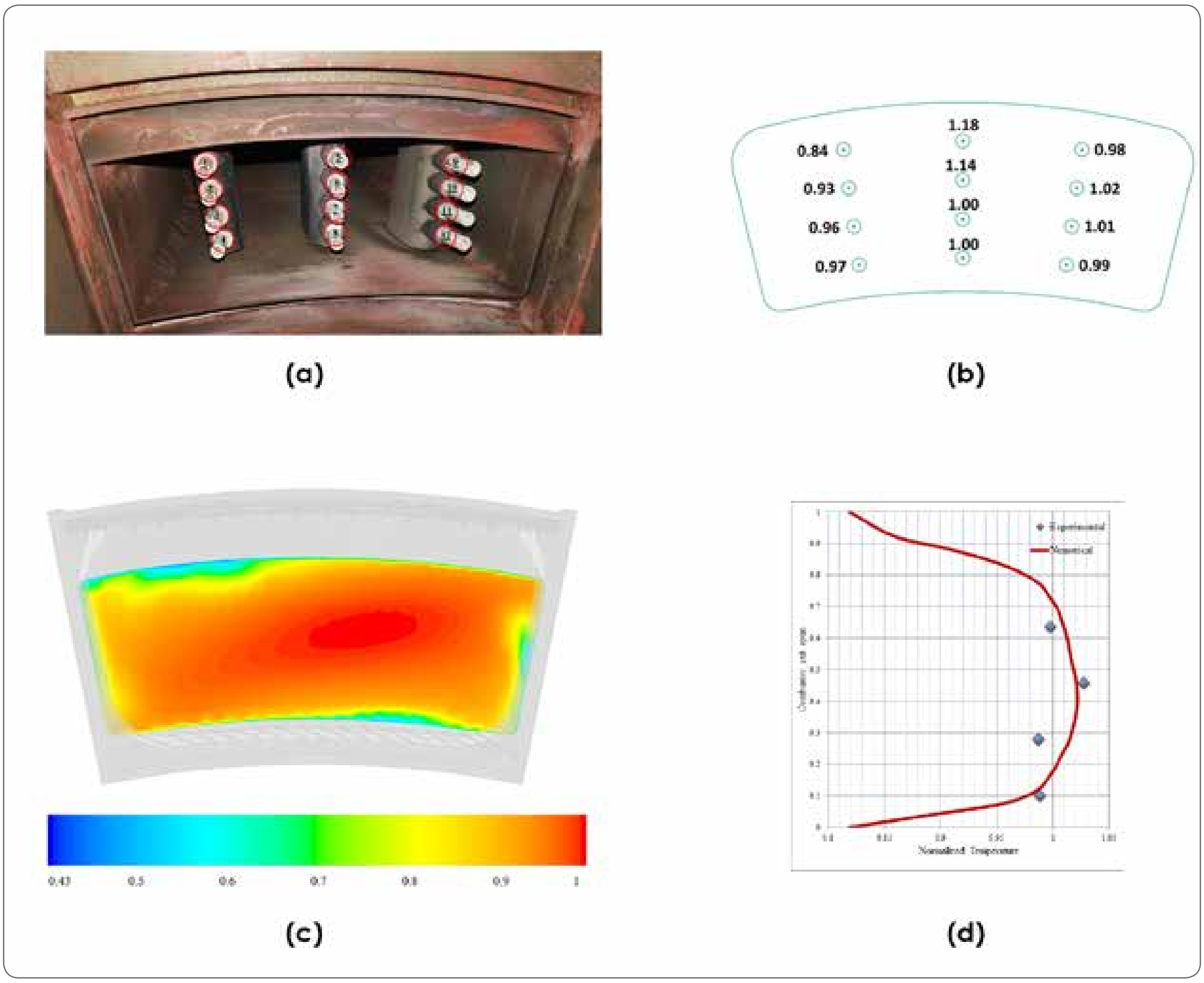

Fig. 6 – DLE combustor exit temperature distribution @ PFR=20%, a. Thermocouple Rake arrangement, b. Normalized gas temperature, c. Normalized gas temperature distribution obtained by CFD, d. Combustor exit averaged gas temperature profile

6

Performance Data-Based Dynamic Modeling for an Industrial Gas Turbine

Introduction

Service companies are in charge of carrying out repairs and upgrading operating systems during specific time periods. Sometimes there are no codified or standard technical documents available for such equipment and hence service companies encounter problems in fulfilling their objectives of providing maintenance, repair and upgrading services.

Designing and testing of control systems, developing online condition monitoring systems and fault diagnosis are entirely dependent on the accuracy and response speed of the dynamic models. The main operating modes of a gas turbine include start-up, loading, and lifting modes each representing specific dynamic features.

Upgrading of logic operation and turbine control system is of paramount importance for repair and maintenance purposes, increased lifetime of the equipment and system upgrades which requires a sound knowledge of turbine operation conditions at different operational modes. In this regard, providing a validated dynamic model is considered as a significant step forward. Turbine shaft speed and its rate of change are the most fundamental parameters in the start-up mode which can lead to the determination of other features of the operating parameters. In order to reproduce the dynamic model of the gas turbine in question at different operational modes including lifting and loading, the operational data obtained from a typical power plant connected to the grid was used. With due attention to the environmental conditions of the operating site, the effects of temperature variations and ambient pressure were also considered on its performance.

The gas turbine under investigation was a single shaft industrial gas turbine with power output of around 40 MW utilized in rather large numbers in the petrochemical industries located in Assaluyeh in the northern coast of Persian Gulf, south of Iran. The dynamic model of this gas turbine is presented in Fig. 1, with similar construction to the Rowen model.

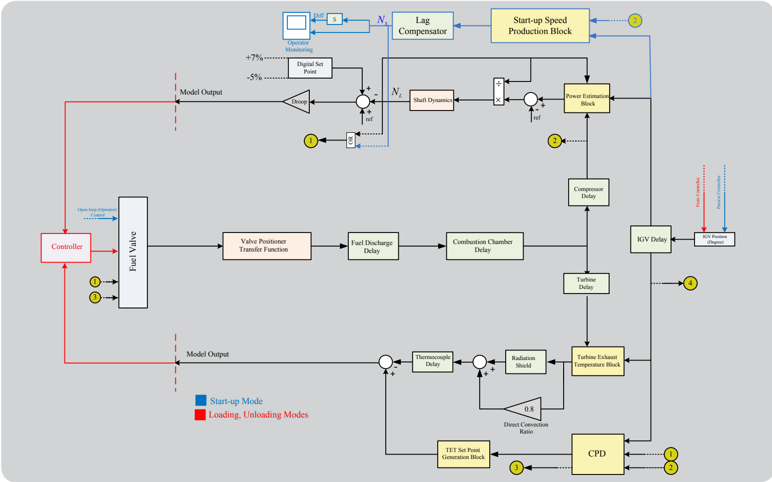

Fig. 1 – Gas turbine dynamic model structure

Modeling

Gas turbine dynamics is a function of the operation of its fuel system. So, regarding the main operating modes, investigating the behavior of the fuel valve is of critical importance for production of the dynamic model of the gas turbine. Thus, the dynamic model is presented in three parts including modeling of fuel valve, start-up and loading modes. Simulation of the valve is carried out in two design states and out of the point. In most of the previous researches carried out in the field of gas turbine dynamic models, the operating construction of the fuel valve had not been considered. In such conditions, the designed controller just produces the signal of the fuel valve for sending the amount of required fuel in terms of percentage values. In the present study, simulation of the fuel valve is performed in a complete form. Proposed information for modeling of the fuel valve has been in the form of a flow coefficient (CV) curve in terms of the position of the GCV[1] valve. A linear function for which the coefficients are achieved by paying due attention to the extracted information from the condition monitoring system is also used for the SRV[2] valve.

The fuel valve of the gas turbine under investigation is comprised of two valves known as SRV and GCV which in order to simulate these valves; ISA standard equations have been used. Simulation results of the fuel valve are demonstrated in Fig. 2. There is a higher sensitivity to the rate of fuel being sprayed during the start-up process. That's why more tested points with less time duration are considered for validation purposes at this stage.

From Fig. 2(b), it is clear that unlike the start-up mode, the rate of pressure changes for the SRV and GCV valves are linear in the loading phase.

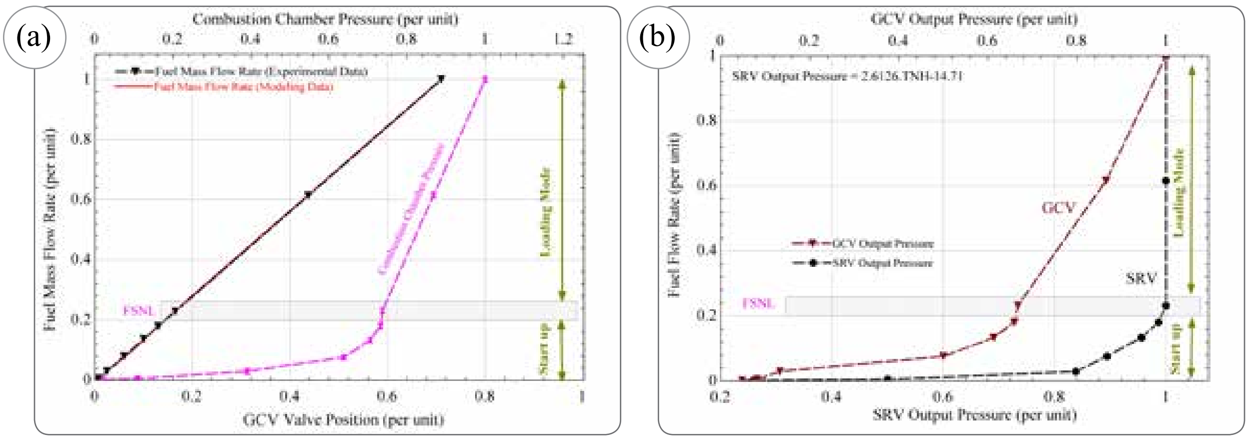

Fig. 2 – Validation of the fuel valve modelling

[1] Gas Control Valves
[2] Stop/Ratio Valve

The start-up mode is an open loop control mode which is performed in a time process. There are significant variables involved in the start-up mode and increasing of the shaft speed does not have a linear relation with increasing fuel discharge. Fig. 3 displays a relationship between input and output variables as well as the role of uncertainties in the production of the system output.

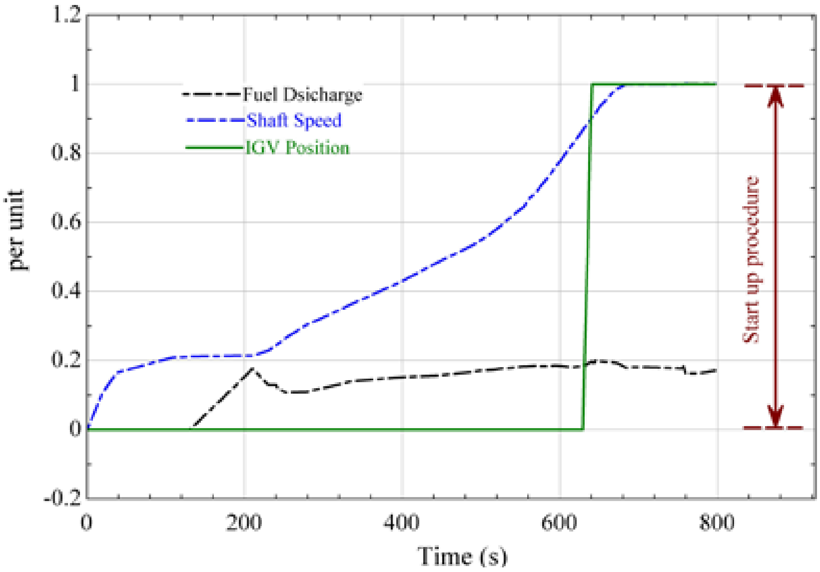

Fig. 3 – IGV position, shaft speed and fuel flow rate in the start-up mode

Two input parameters including the rate of fuel sprayed as well as the IGV position were among available information for dynamic modeling of the gas turbine under investigation. For system simulation in such conditions, the combination of linear and nonlinear equations of system inputs accompanied by dynamic delay transfer functions was used in order to achieve acceptable precision. In doing so, several different scenarios were considered for production of the outputs. In the first scenario, with due attention to the significant advantages of neural networks in nonlinear equation production, they got used to reproduce the relationship between the existing variables.

In the second scenario, the linear regression method was used. The obtained functions were presented in three different operating modes including close IGV, open IGV and opening stage of the IGV. In the third scenario, fuel discharge and shaft dynamics were used as input parameters to the shaft conversion function. Finally and for the third scenario, the identification methods namely HW and NARX were used to reproduce the relationship between the input and output of the system.

These methods can be significant options in the estimation of system behavior because of the application of time delays. Due to the effects of uncertainties on system outputs, functional behavior of the system was affected and an unknown behavior was occurred in higher regimes especially at speeds of over 70%. The reason for this phenomenon is the IGV variable presence and uncertainties due to the blades and shaft inertia. Subsequently and in order to cover system uncertainties, time delay functions were presented. These functions are delay (lag) compensators that their coefficients are presented with due attention to correspondence value with reference operating plot for each of scenarios (Table 1).

[1] Hammerstein-Wiener

[2] Nonlinear Auto-Regressive Exogenous

Table 1: Lag compensators

Method	NARX	HW	NN[3]	SD[2]	LR[1] IGV=0	LR[1] IGV=1
Transfer function	$\frac{70s + 5.189}{1000s + 2.7}$	$\frac{300s + 1.085}{1000s + 2.7}$	$\frac{50s + 1.031}{1000s + 2.7}$	$\frac{120.45s + 0.186}{600s + 0.13}$	$\frac{-250s - 1.185}{500s + 0.23}$	$\frac{2010s+0.9246}{500s + 0.23}$

After applying the converted interaction, the output behavior of the system is modified, as shown in Fig. 4.

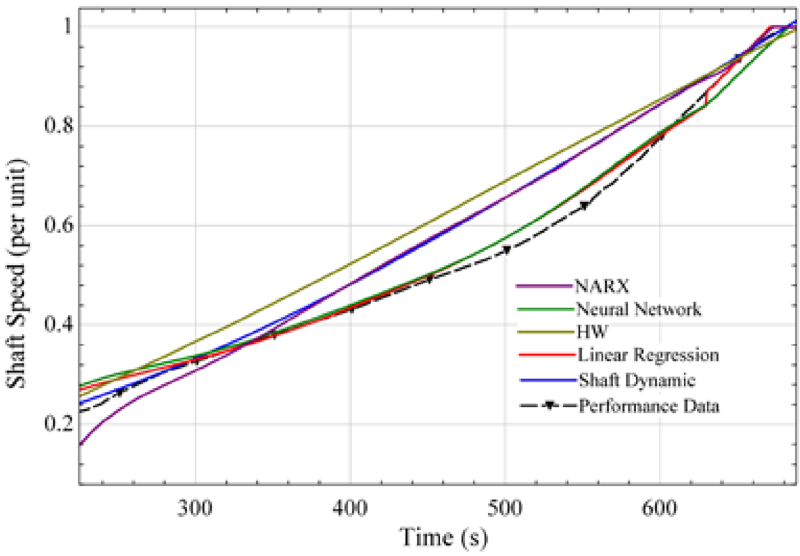

Fig. 4 – Compensator effects on proposed methods

The most important external disturbances entailed in the system are changes in the fuel heat rate value and environmental conditions. In order to investigate the effects of fuel heat rate turbulence on the results of the neural network method, related output graphs were studied in the range of 10% of variations in fuel discharge. Among the scenarios presented and according to the logical conformance to system conditions, the preferred methods in order are neural network, NARX, shaft dynamics, linear regression and HW methods.

In order to improve and adapt the neural network method as a selective method, it is necessary to determine the effect of fuel heat rate on the amount of shaft speed distortion independently. The best way to find most suitable points for determining the best operation matching the model with the system is using an operating trend where there is roughly a linear relationship between the fuel spray rate and shaft speed. With respect to the points given, a relationship between the shaft speed and fuel rates could be found. Due to distance from the modified function line, the coefficient for the input fuel can be re-established. Finally, using modified coefficients for minimum and maximum heating rates, a modified diagram is achieved, shown in Fig. 5.

[1] Linear Regression
[2] Shaft Dynamic
[3] Neural Network

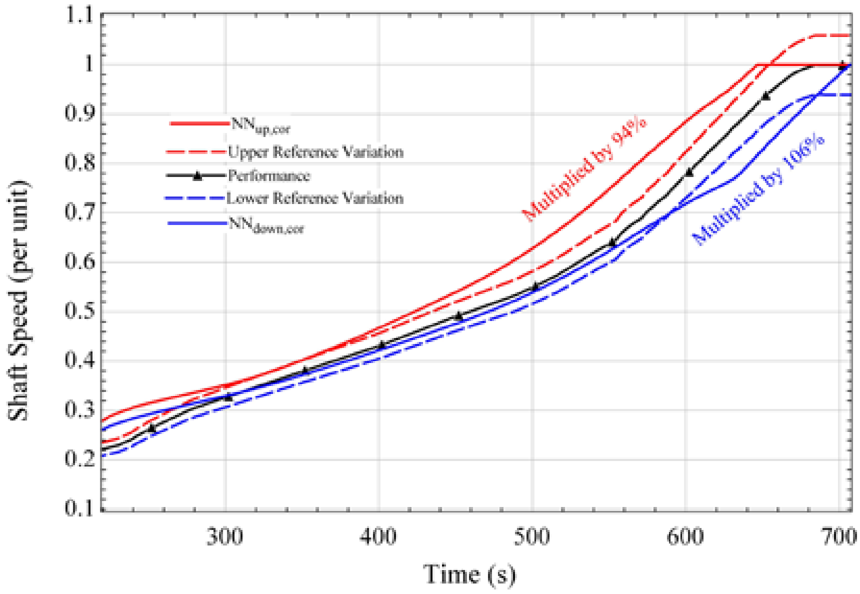

Fig. 5 – Corrected neural network method outputs in comparison with real performance trends

One of the other important control parameters is the Turbine Exhaust Temperature (TET). In order to obtain the function associated with this parameter, a linear two variable function with maximum possible accuracy is used. A diagram representing behavior of the model with different shaft speeds and fuel heat rates in comparison with the actual performance of the machine is presented in Fig. 6(a). Also a linear two variable function based on three main variables of the IGV position, fuel heat rate and turbine shaft speed is extracted for the Compressor Pressure Discharge (CPD), as presented in Fig. 6(b) for different shaft speed and fuel heat rate values.

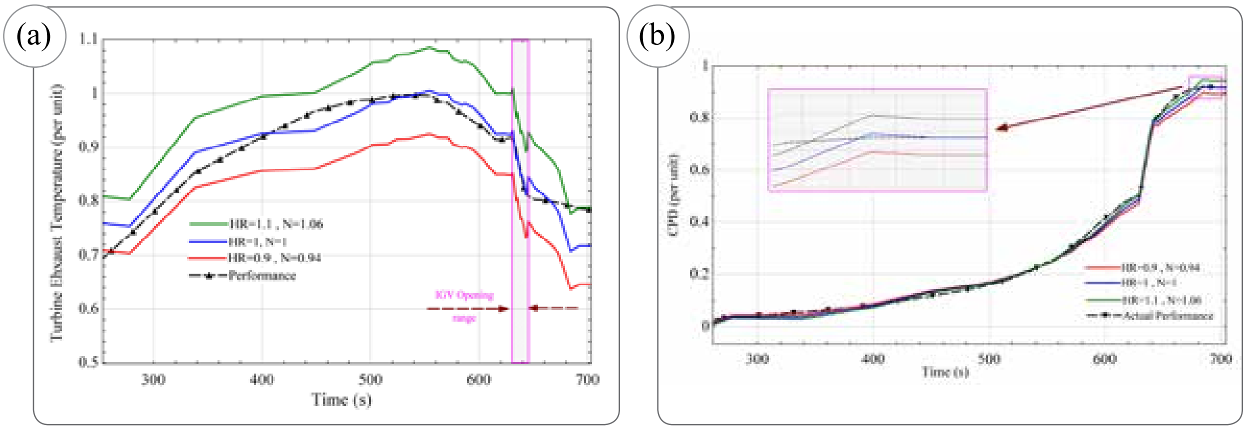

Fig. 6 – Obtained TET and CPD functions based on different shaft speeds and fuel heat rates

In addition to the thermal effects of the input fuel heat rate, impacts of the environmental factors on the outputs of the system are also important both in the start-up and loading modes. The environmental disturbance of this system, based on its geographic location, only includes environmental temperature. Equation **(1)** is used to take into account the effect of temperature change and calculation of the modified shaft speed.

$$n_{new} = n_{ref}\sqrt{\frac{T_{new}}{T_{ref}}} \quad (1)$$

The temperature of the exhaust gases is also a function of environmental conditions. In this context, Equation (2), which is based on an experimental relation between the ambient and exhaust gas temperatures at ISO conditions, is employed to increase the temperature of the exhaust gases.

$$TET_{new} = TET_{ref} + \frac{(T_{new} - T_{ref})}{TET_{ref}} \quad (2)$$

Loading modes of the system are the most important modules to design the controller since most of functional changes in the system are closed loop controllers. The output power of the system is the most important control parameter during loading of the system. This variable is directly proportional to the input thermal heat rate in the combustion chamber and can be obtained from the fuel heat rate, regardless of the IGV effect with a good approximation (Fig. 7). Calculated output power is plotted in Fig. 7 for different heat rate values.

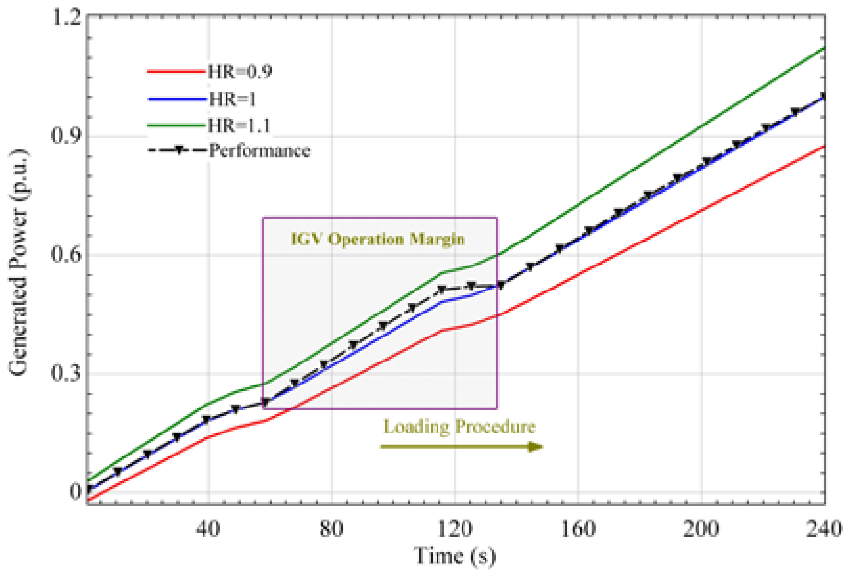

Fig. 7 – Obtained generated power function for several different heat rate values

One of the other most important variables for designing and adjusting the system is temperature control for the exhaust gases from the turbine, especially in hot environments. In addition to the fuel, this variable is also a function of the IGV position. The temperature of the exhaust gases is defined as a linear function of the input variables. The simplicity of the obtained function is an advantage for the response time and model speed (Fig. 8(a)).

The last function required for the dynamic model to be completed is the compressor pressure discharge. For closed IGVs and open IGVs, one function is used, and the pressure ratio is a function of the fuel heat rate and the IGV opening value. Regarding the obtained graphs (Fig. 8(b)), the part of the diagram that has been removed from the baseline mode needs to be corrected. Therefore, in the IGV function range, using constant coefficients, it is possible to modify the state of the lower than or greater than the reference value respectively and reach the logical values.

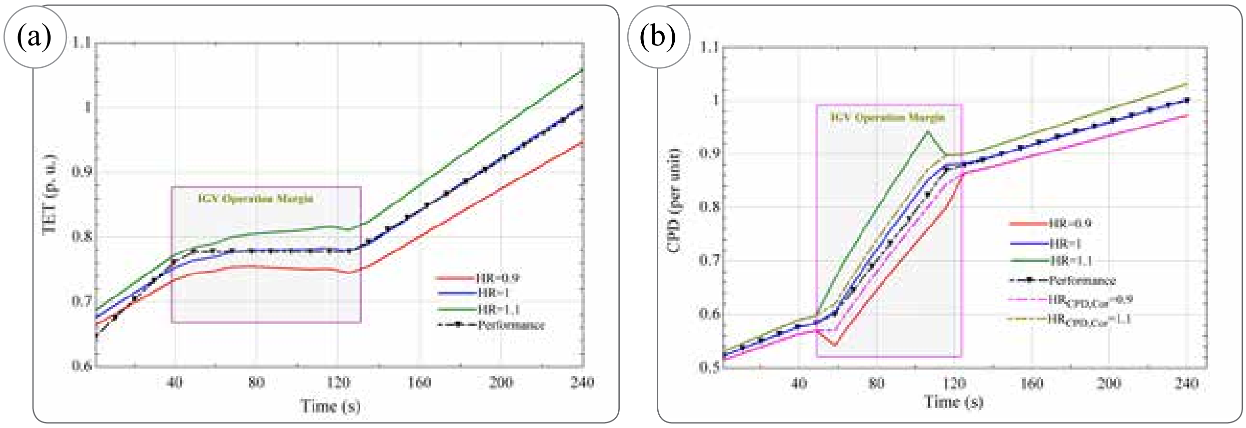

Fig. 8 – Obtained CPD and TET functions for different fuel heat rate values

In addition to the temperature of the exhaust gases, in case of loading mode, the power output of the turbine is introduced as a variable influenced by the environmental conditions. In the developed model, using the relationship between the density and the air temperature, a simpler equation which has a smaller number of variables is used.

Concluding Remarks

The main objective of this investigation was to provide a reliable dynamic model in different modes using the monitoring system data. In the developed model, all disturbances and possible uncertainties were examined and the outputs of the model were presented with acceptable accuracy. The results of the start-up mode represent relative superiority of the neural network method to generate turbine output speed. In loading mode, however, due to simplicity and speed of the extracted functions, the functions derived from linear regression method were used to generate the dynamic model.

Head Office:
231 Mirdamad Ave. Tehran, I.R.Iran.
P.O.Box: 15875-5643
Tel: +98 (21) 22908581
Fax: +98 (21) 22908654

Factory:
Mapna blvd., Fardis, Karaj, I.R.Iran.
Post code: 31676-43594
Tel: +98 (26) 36630010
Fax: +98 (26) 36612734

www.mapnaturbine.com
tr@mapnaturbine.com

The technical and other data contained in this Technical Review is provided for information only and may not apply in all cases.

GR295-0